A drug delivery system based on poly-L-lysine grafted mesoporous silica nanoparticles for quercetin release

Cristina Carucci[1,2], *Giulia Sechi*,[1] *Marco Piludu*,[3] *Maura Monduzzi*,[1,2] *Andrea Salis*[1,2]

[1]*University of Cagliari, Department of Chemical and Geological Science, Cittadella Universitaria, 09042 Monserrato-Cagliari, Italy*

[2]*Consorzio Interuniversitario per lo Sviluppo dei Sistemi a Grande Interfase (CSGI), via della Lastruccia 3, 50019, Sesto Fiorentino (FI), Italy.*

[3]*Dipartimento di Scienze Biomediche, Università di Cagliari, Cittadella Universitaria, SS 554 Bivio Sestu, 09042 Monserrato, CA, Italy*

ABSTRACT

Mesoporous silica nanoparticles (MSN) functionalized with aminopropyl-triethoxysilane (NH_2), triethylenetetramine (TETA) and poly-L-lysine (PLL), were loaded with the flavonoid quercetin to obtain a potential antimicrobial drug delivery system. The systems were fully characterized by means of several techniques. Quercetin loading and release were investigated in different conditions using the diverse functionalized MSN. Quercetin loading was checked for MSN, MSN-NH_2 and MSN-TETA using EtOH:H_2O mixtures at ratio 80:20 and 50:50. Although loading was higher using the 80:20 solvent mixture, a more efficient release was ascertained using the solvent mixture 50:50 as demonstrated by experimental release kinetics. The constant release rate k_1, determined at physiological pH, decreased in the order MSN > MSN-NH_2 > MSN-TETA suggesting a stronger interaction of deprotonated quercetin with positively charged moieties of functionalized MSN. The maximal concentration of released drug A_{max} was achieved for MSN-TETA system. PLL-grafted MSN systems were loaded with quercetin using the 50:50 EtOH:H_2O solvent mixture. The k_1 values were slightly higher with respect to those found for MSN-NH_2 and MSN-TETA, likely due to the preferential adsorption of quercetin at the particle external surface. Nevertheless, A_{max} values for MSN-NH_2-PLL and MSN-TETA-PLL were in the concentration range (0.2-3 μg/mL) found in plasma after quercetin oral administration. MSN-TETA-PLL system, in agreement with the significant dependence of its zeta potential on pH, allowed for a higher release at pH = 3 compared to pH = 7.4. Finally, a stability up to six hours of incubation, for quercetin loaded into PLL-grafted MSN, was ascertained through UV-Vis spectroscopic analysis, thus suggesting a good protective effect of functionalized MSN against oxidation that, as for other flavonoids, quickly occurs at physiological pH.

*Corresponding authors: Dr. Cristina Carucci cristina.carucci@unica.it, Prof. Andrea Salis asalis@unica.it

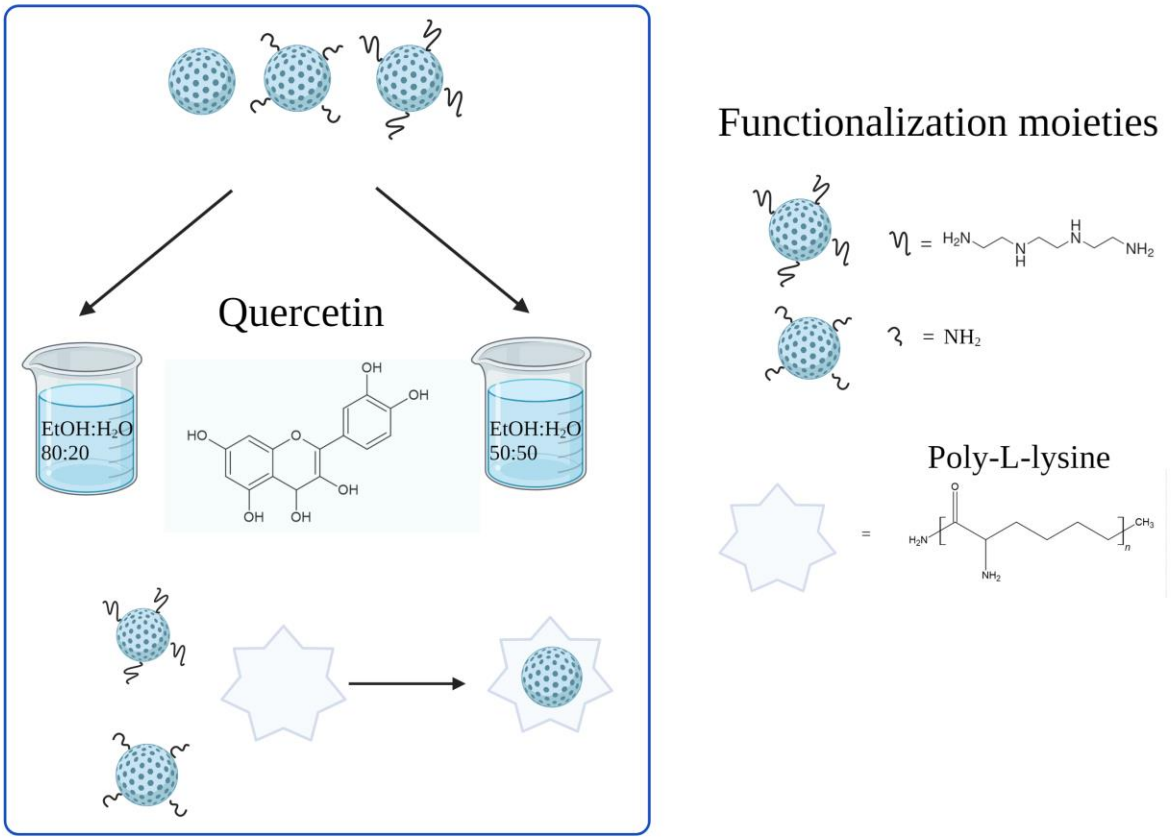

GRAPHICAL ABSTRACT: Quercetin loading with two EtOH:H_2O mixtures on MSN, MSN-NH_2, MSN-TETA. Functionalization on MSN-NH_2, MSN-TETA to obtain MSN-NH_2-PLL and MSN-TETA-PLL.

1. Introduction

The increasing demand of new drugs and smart drug delivery systems (DDS) to counteract antibiotic resistance has promoted wide-ranging research approaches to produce versatile and tunable DDS platforms, often based on hybrid multifunctional nanomaterials.[1,2] The choice of functionalized nanostructured drug carriers allows to protect and transport drugs to the desired target at the appropriate concentration.[3–5] Among a wide range of nanomaterials used to this purpose (i.e. polymeric micelles,[6] liposomes,[7] iron oxide nanoparticles[8]), significant advances have been achieved through the use of functionalized mesoporous silica nanoparticles (MSN) and antimicrobial agents such as flavonoids and polypeptides.[9,10] Indeed, mesoporous silica nanoparticles (MSN) are one of

the most promising nanocarriers thanks to their peculiar features, such as high surface area (up to 1000 m^2/g), narrow pore size distribution and easy surface functionalization.[11–15] However, bare silica nanoparticles have low biocompatibility.[16] Furthermore, due to weak surface interactions between the silica and many drug molecules, bare MSNs often suffer of burst drug release.[17–19] To overcome these drawbacks, MSNs can be functionalized with a wide range of chemical moieties[20] and polymers.[5,21,22] Among polymers, cationic antimicrobial peptides (AMP) have been recognized to be very promising against multi-drug resistant bacteria and fungi.[1,2,5,23] Among diverse AMPs, poly-L-lysine (PLL), in addition to its potential as antimicrobial agent, characterized by low cytotoxicity, biocompatibility and biodegradability, provides stimuli responsive properties.[24] Indeed, due to pK_a around 9 of amino groups, PLL under physiological condition at pH ≈ 7, is positively charged.[25] Hence, PLL-grafted MSN have been studied as water soluble cationic pH responsive drug delivery systems.[26,27] PLL functionalized MSNs have been used against cancer cells. For example Lio et al. found that PLL coated MSNs were highly efficient to penetrate the skin for transdermal delivery of Si-RNA against skin cell carcinoma.[28] Hartono et al. demonstrated how PLL functionalized MSN was a superior carrier when compared with MSN-NH_2 for the transport and release of genes against osteosarcoma cancer cells especially by enhancing cellular uptake.[29] PLL grafted MSN have been used also against bacteria. Dai et al.[30] grafted PLL on MSN loaded with copper sulfide nanoparticles to contrast the bacterial activity of *P. aeruginosa* and *S. aureus.*

Quercetin (5,7,3,4'-hydroxyflavanol) is a flavanol found in a wide range of plants[31] and food products such as onions, berries, and cilantro.[32] Among its numerous properties such as anti-inflammatory,[33] antineoplastic[34] and antioxidant activity[35] quercetin has been recently evaluated for its antibacterial[36] and antiviral[37] uses. Quercetin antibacterial mechanism is due to destruction of plasma membrane and inhibition of bacteria's nucleic acid synthesis.[38,39] More recently free quercetin has been studied as a possible antibiotic alternative.[40] Unfortunately, quercetin shows low bioavailability and limited cellular absorption due to its low solubility in water.[41,42] In addition, quercetin suffers of high photo- and thermo-sensitivity which makes it difficult to use for biomedical applications except when taken

at high oral doses (200-500 mg three-five times a day).[42,43] Loading quercetin on MSNs helped to overcome this issue for topical administration in the use of creams and ointments.[44] Berlier et al. loaded quercetin on MSNs functionalized with octyl groups to study its topical use to prevent skin damage from light.[45] MSN-NH_2 were also studied as carriers for topical quercetin delivery.[46] Quercetin loaded MSNs have also been studied as a potential anti-cancer DDS, as in the work by Sarkar et al. which found that quercetin-loaded MSNs functionalized with folic acid induced apoptosis in breast cancer cells.[47]

Due to its low solubility, both impregnation and adsorption procedures have been studied to optimize quercetin loading on MSNs.[42,46,48,49] For example, Sapino et al.[46] used the impregnation method dissolving quercetin in methanol for drug topical delivery. Ghanimati et al.[48] studied the adsorption of quercetin from water–ethanol (0-100%) mixtures achieving high drug loading values at basic pH. Rubini et al. compared the loading of quercetin on gelatin films by dissolution in either DMSO or EtOH:H_2O (50:50) mixtures.[49] Kazakova et al. found that increasing the EtOH content in a EtOH:H_2O mixtures increased quercetin solubility at the expense of quercetin adsorption on silica NPs.[50] While the effect of solvent mixture composition was often studied to maximize quercetin loading in carriers,[46,48–52] to the best of our knowledge, no studies have investigated its effect on the following quercetin release from MSN.

Herein, a hybrid nanostructured stimuli responsive DDS based on quercetin loaded on PLL-functionalized MSNs was prepared. MSNs were characterized through TEM, SAXS, FTIR, TGA, ELS and N_2 adsorption/desorption isotherms. Functionalization to introduce propyl-NH_2, TETA (triethylenetetramine) and PLL moieties, was performed. The effect of EtOH:H_2O mixture composition (80:20 and 50:50) on quercetin loading on MSNs, MSN-NH_2 and MSN-TETA was investigated. Then, quercetin release under physiological conditions for the DDS obtained from two EtOH:H_2O solvent ratios used in the loading step, was quantified along with the release dependence

on functionalization moiety. Finally, the PLL grafted samples were investigated to evaluate quercetin stability together with the optimal release concentration.

2. Materials and methods

2.1 Reagents

Hexadecyltrimethylammonium bromide (CTAB > 99%), tetraethoxysilane (TEOS 98%), toluene (99.8%), 3-aminopropyl-triethoxysilane (APTES > 98%), triethylenetetramine (TETA ≥ 97%), NaH_2PO_4 (99%), Na_2HPO_4 (99%), NaCl, NaOH pellets, (3-chloropropyl)trimethoxysilane (CPTMS ≥ 97%), ammonium nitrate (NH_4NO_3 99%), HCl (37%), quercetin HPLC grade (≥ 95%), dimethylformamide (DMF ≥ 99,9%), aqueous glutaraldehyde (50%), poly-L-lysine hydrobromide (mol wt 15000-30000) were all purchased from Sigma Aldrich (Italy). Ethanol (99.8%) was purchased from Honeywell.

2.2 MSN synthesis and functionalization

MSN synthesis was carried out following a published protocol which provides MSN grafting prior CTAB removal.[13] (see details and physico-chemical characterization in Supporting Information).

2.3 Quercetin loading on bare and functionalized MSN

Quercetin loading was performed with two EtOH:H_2O mixtures at two different ratio. For mixture 80:20 EtOH:H_2O MSN, MSN-NH_2, MSN-TETA, MSN-NH_2-PLL and MSN-TETA-PLL were loaded by soaking 120 mg of each sample in 12 mL of a quercetin solution (10 mg/mL). For mixture 50:50 EtOH:H_2O, MSN, MSN-NH_2, MSN-TETA, MSN-NH_2-PLL and MSN-TETA-PLL were loaded by soaking 50 mg of MSN in 2 mL of a quercetin solution (2.5 mg/mL). All suspensions were stirred on a rotational shaker at 15°C for 24 h. All suspensions were then centrifugated and the supernatant removed. Materials were all dried under vacuum prior use. To determine drug loading on MSN, the supernatant concentration was determined by measuring the absorbance at 375 nm (final

drug concentration) using the appropriate calibration curve (in range of 0.05 mg/mL-2.5 mg/mL for 50:50 EtOH:H_2O solutions and 0.5 mg/mL-10 mg/mL for 80:20 EtOH:H_2O solutions). Drug loading was calculated by the equation:

$$Drug\ loading(\frac{mg}{g}) = \frac{([D]_i - [D]_f)V}{m} \quad (1)$$

Where, $[D]_i$ and $[D]_f$ are the initial and final drug concentrations (mg/mL), respectively. V is the volume of drug solution (mL) and m is the mass of the MSN carrier (g).

2.4 Kinetics of quercetin release

To study quercetin release a mass of 50 mg of quercetin loaded sample were dispersed in 50 mL of phosphate buffer saline (PBS) 100 mM, NaCl 150 mM at pH 7.4. Each sample was stirred (156 rpm) and incubated at 37°C. After 1 h, 2 h, 3 h, 4 h, 5 h, 6 h and then after 24 and 25 h, 3.5 mL of sample were collected and immediately replaced with the same volume of fresh PBS solution to maintain *sink conditions*.[53] The amount of drug released was determined at wavelength of 375 nm. The same measurement was performed at pH 3 and pH 7.4 for MSN-NH_2-PLL and MSN-TETA-PLL to evaluate PLL responsive properties. PBS at both pH to avoid the use of a different buffer as reported for MSN-PLL gatekeeper.[54]

$$Drug\ \ concentration(\frac{\mu g}{mL}) = A_{max}(1 - e^{-k_1 t}) \quad (2)$$

The quantity of released quercetin has been calculated according to equation 2, where drug concentration represents the amount of drug released at specific time (μg/mL), A_{max} is the maximal concentration of released drug (μg/mL) and k_1 (h^{-1}) is the release constant rate

2.5 Quercetin stability

Quercetin at concentration 2 μg/mL were dissolved in PBS buffer 100 mM, NaCl 150 mM, at 37°C at pH 3 or at pH 7.4. Immediately after preparation, after 6 h and 24 h of incubation 3.5 mL of sample were withdrawn and UV-vis spectra were registered from 200 to 800 nm. Release spectra of quercetin

from MSN-NH_2, MSN-TETA, MSN-NH_2-PLL and MSN-TETA-PLL were registered in the same wavelength range after incubation in the same conditions.

3. Results and discussion

3.1 Characterization of MSN, MSN-NH_2 and MSN-TETA

Synthesized MSNs were characterized by TEM, SAXS and N_2-adsorption techniques. TEM images in Fig. 1 (A-B) show MSNs particles having ellipsoidal shapes with an internal structure constituted by typical parallel channels. SAXS pattern of MSNs in Fig. 1C displays an intense peak relative to the reflection of the 100 plane and three less intense peaks due to 110, 200 and 210 planes. This pattern confirms the occurrence of an ordered 2D hexagonal phase with a lattice parameter a = 47 Å. The functionalization of the external surface of MSNs of propyl-NH_2 and TETA moieties to obtain MSN-NH_2 and MSN-TETA samples, respectively, was carried out before CTAB extraction as previously reported.[55] MSN were characterized by FTIR spectroscopy. All samples show the characteristic peaks around 1060 cm^{-1} and 800 cm^{-1} due to the stretching vibrations of Si-O-Si bond (Fig. S1). Successful post functionalization CTAB extraction was confirmed by the disappearance of C-H stretching bands at 2922 cm^{-1} and 2853 cm^{-1}. MSN-CTAB-NH_2 and MSN-NH_2 spectra show -NH_2 bending at 1560 cm^{-1}. To obtain MSN-TETA sample, the grafting of the propyl-Cl moiety is needed as first step leading to the synthesis of MSN-CTAB-Cl. MSN-CTAB-Cl synthesis is confirmed by the clear disappearance of silanol peak at 970 cm^{-1}. The so functionalized MSN was then treated with TETA. MSN-CTAB-TETA and MSN-TETA spectra show a band at 1654 cm^{-1} due to the NH_2 bending (Fig. S1). The structural order typical of MCM-41 materials[56] is retained after propyl-NH_2 and TETA functionalization as confirmed by the SAXS patterns showing the hexagonal phase (Fig. 1C) and the unaltered lattice parameter values (Table 1). MSN sample has a BET surface area of 1142 m^2/g which decreases for MSN-NH_2 and MSN-TETA sample to 630.3 and 717.2 m^2/g, respectively. A slight decrease of pore size from 2.8 nm (MSN) to 2.5 nm (MSN-NH_2) and 2.3 nm (MSN-TETA) is shown. While there is not functionalization present within the pores, surface area

and pore size decrease could be due to a partial closure of pore openings consequent to the external functionalization on MSN surface.

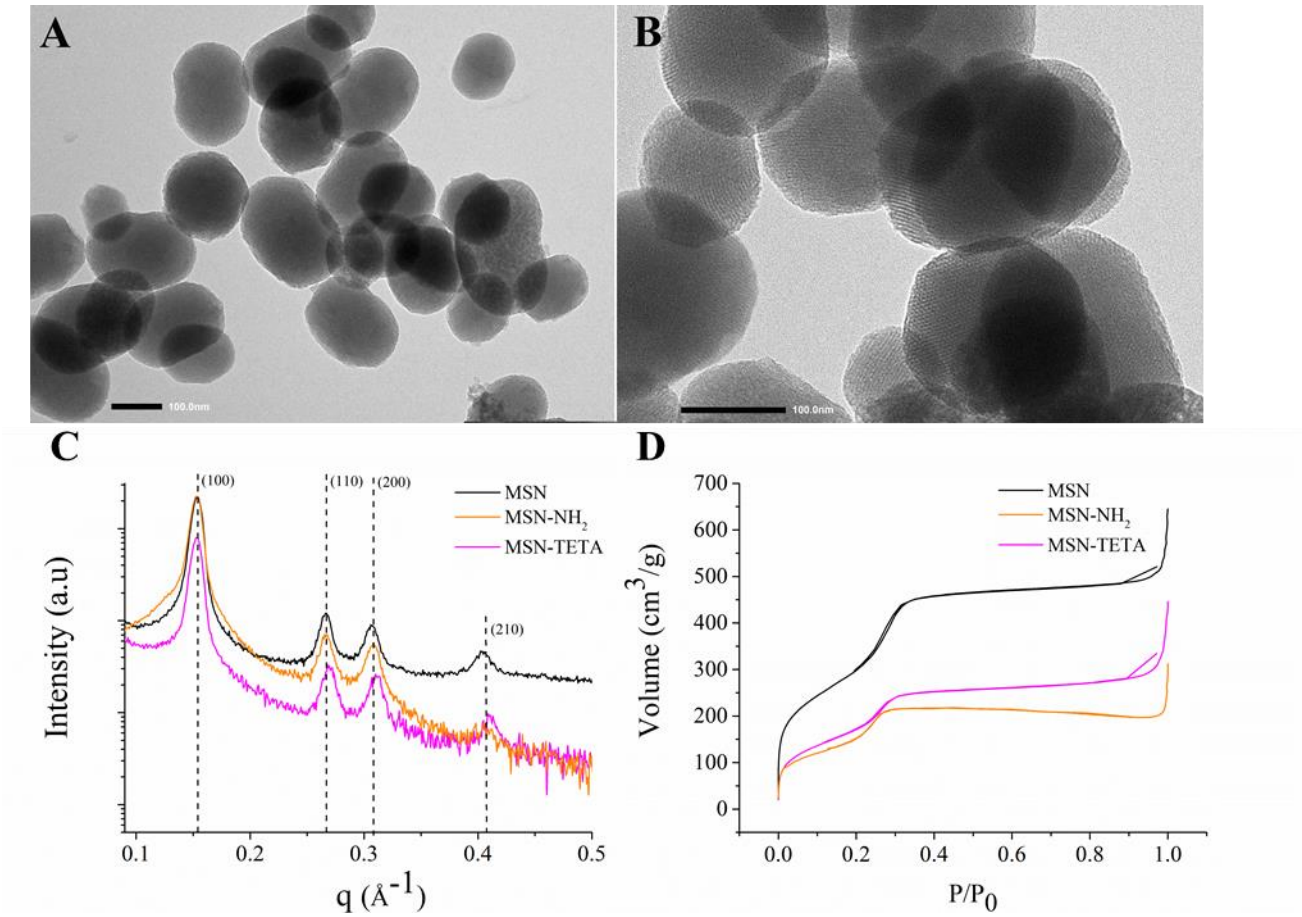

Figure 1. TEM images of MSN at different magnifications A-B) structural characterization of MSN, MSN-NH_2 and MSN-TETA as C) SAXS patterns D) adsorption/desorption N_2 isotherm.

Table 1. Samples characterization data.

Sample	[a]S_{BET}(m^2/g)	[b]V_P (cm^3/g)	[c]d_P (Å)	[d]*a* (Å)
MSN	1142	0.9	28	47
MSN-NH_2	630	0.4	25	47
MSN-TETA	717	0.6	23	47

[a] Surface area calculated by BET method, pore volume from the desorption branch calculated at P/P_0=0.99 by BJH method, [b] pore volume and [c] pore diameter calculated with BJH method to the isotherm desorption branch, [d] lattice spacing of MSNs calculated with the equation $a_{(hex\ phase)} = (2/3^{0.5})\times(h^2 + k^2 + l^2)^{0.5}$.

To confirm nanoparticles functionalization, TG analysis of MSN in comparison with MSN-NH_2 and MSN-TETA samples was performed (Fig. 2). Mass losses < 100° C are attributed to the loss of humidity. In the temperature range between 100 °C and 250 °C a mass loss of 12.1% and 7.9% attributed to the organic moieties of MSN-NH_2 and MSN-TETA, respectively. The mass losses for

MSN-NH_2 and MSN-TETA at 250°C are likely due to the sole MSN external functionalization. This might provoke a net loss of the propyl-NH_2 and triethylenetetramine moiety which causes a sudden drop in mass. These mass losses correspond to an amount of grafted functional group of 110.8 mg/g for MSN-NH_2 and of 76.8 mg/g for MSN-TETA (Table 2). PLL modification is confirmed by thermal degradation beginning at 250-575 °C with a mass loss of 20 % and 27.4% for MSN-NH_2 and MSN-TETA respectively.

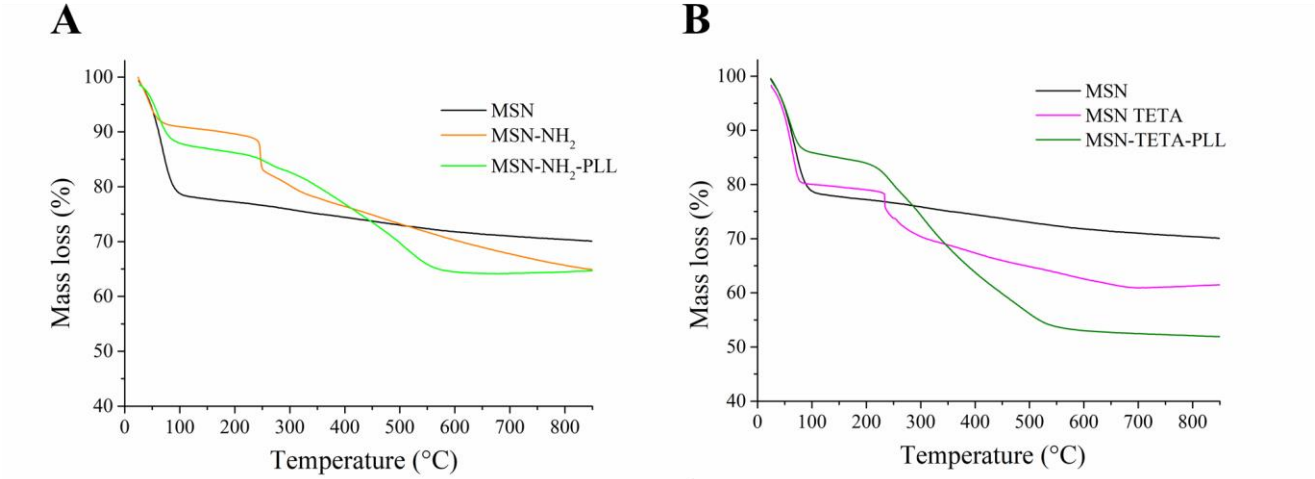

Figure 2. Thermogravimetric analysis of A) MSN, MSN-NH_2, MSN-NH_2-PLL and B) MSN, MSN-TETA, MSN-TETA-PLL.

Table 2. Mass losses % and amount of grafted functional groups (mg of moiety per g of MSN) calculated from TGA data for functionalized MSN samples. Isoelectric point (pI) from zeta potential measurements (Fig. 4)

Sample	25 °C < T< 100 °C	100 °C < T < 250 °C	250 °C < T< 575 °C	Func. moiety (mg/g)	pI
MSN	21.6	-	-	-	4.2
MSN-NH_2	8.8	12.1	10.0	110.8	7.9
MSN-NH_2-PLL	13.1	2.5	20.0	100.3	8.3
MSN-TETA	20.2	7.9	13.4	76.8	9.1
MSN-TETA-PLL	15.5	6.7	27.4	140.7	9.8

3.2 Quercetin loading and release from MSN, MSN-NH_2, MSN-TETA

Drug loading on MSNs can be obtained by impregnation or adsorption methods or a combination of both. In the former, a solvent where the drug is highly soluble is used. The solvent must also have a

low surface tension, so that it can easily evaporate leaving the drug inside the mesopores. In the latter, the drug should not have a high solubility in the solvent, otherwise the establishment of attractive interactions with the particles' surface would be unfavored. Sometimes both impregnation and adsorption phenomena are simultaneously at work. Although the effect of the solvent on drug loading is usually considered, the successive effect on the release has not been deeply investigated yet. For example, Popova et al. used the impregnation method by dissolving quercetin in pure ethanol.[57] They obtained a burst release (60% of drug mass in 30 mins) from bare silica particles, likely because of the lack of attractive interactions between quercetin and the silica surface. In our case quercetin loading on MSNs was firstly carried out dissolving the drug in a mixture of EtOH:H_2O 80:20 (v/v). This solvent mixture result in a quercetin loading, quantified by UV-Vis analysis, corresponding to 627.6 mg/g for bare MSNs, and 98.2 mg/g for MSN-NH_2 and 347.6 mg/g for MSN-TETA (Table 3). A mixture of EtOH:H_2O 50:50 (v/v) was also used to load quercetin. The lower ethanol content in the solvent mixture resulted in a lower quercetin loading for all samples, with the highest obtained for MSN-TETA (92.8 mg/g) and MSN-NH_2 (92.6 mg/g) and the lowest for bare MSNs (80.4 mg/g). The higher quercetin loading obtained for EtOH:H_2O 80:20 mixture is consistent with a process in which impregnation prevails on adsorption. This result is also in agreement with what reported in the literature.[50]

Table 3. Effect of solvent mixture composition (EtOH:H_2O 80:20 and EtOH:H_2O 50:50) on quercetin loading and release (kinetic parameters: A_{max}, k_1 and R^2 calculated by fitting equation 2) from different MSN samples.

	EtOH:H_2O (80:20)				**EtOH:H_2O (50:50)**			
Release pH 7.4	**Loading (mg/g)**	**A_{max} (µg/mL)**	**k_1 (h^{-1})**	**R^2**	**Loading (mg/g)**	**A_{max} (µg/mL)**	**k_1 (h^{-1})**	**R^2**
MSN	627.6	1.8	80.9	0.93	80.4	3.8	1.3	0.96
MSN-NH_2	98.2	1.8	1.6	0.96	92.6	2.8	0.2	0.90
MSN-TETA	347.6	2.8	2.7	0.98	92.8	5.2	0.1	0.96

The effect of EtOH:H_2O ratio in the loading step on quercetin release was then studied. For samples loaded using 80:20 EtOH:H_2O ratio, the maximal concentration of released quercetin $A_{max,}$ was 1.8 µg/mL for MSN and MSN-NH_2 increasing up to 2.8 µg/mL for MSN-TETA. The release kinetic constant, k_1, was very high for bare MSN (80.9 h^{-1}) suggesting a burst release of quercetin. Lower values of k_1, 2.7 h^{-1} and 1.6 h^{-1}, were obtained for MSN-TETA and MSN-NH_2, respectively. This suggests the occurrence of attractive interactions between quercetin and the functionalized MSNs which slowed down the process making the release more sustained. Although, bare MSNs reached the highest quercetin loading with a solvent composition EtOH:H_2O 80:20, their release performance were very poor both in terms of A_{max} and k_1.

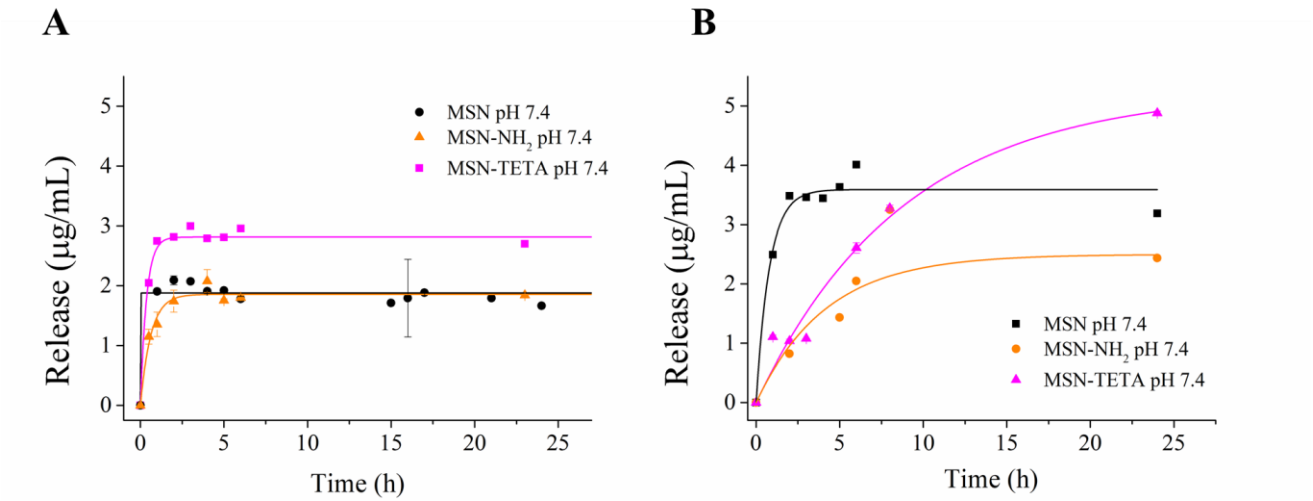

Figure 3. Quercetin release of MSN, MSN-NH_2, MSN-TETA after quercetin loading in a EtOH:H_2O mixture A) 80:20 and B) 50:50.

The use of a solvent composition (EtOH:H_2O 50:50) had the important effect to slow down the quercetin release and to modulate the maximal concentration of quercetin for all MSN samples. Bare MSN showed a fast quercetin release (k_1=1.3 h^{-1}) which was in any case much lower than that obtained for the 80:20 EtOH:H_2O mixture. In addition, both functionalized samples showed much slower release with values of 0.2 h^{-1} and 0.1 h^{-1} for MSN-NH_2 and MSN-TETA, respectively. The decrease of release kinetic constants follows the order of MSN > MSN-NH_2 > MSN-TETA

correlating the occurrence of a more sustained release with surface functionalization and indicating a general better performance of the DDS loaded with a lower ethanol content. $A_{max,}$ was 2.8 µg/mL for MSN and 3.8 µg/mL MSN-NH_2 with MSN-TETA showing the highest A_{max} at 5.2 µg/mL. These results suggest that adsorption is more useful than impregnation as a method to load quercetin on functionalized MSN carriers. Due to the better release performance of samples loaded with EtOH:H_2O 50:50 ratio, this solvent composition was chosen to study quercetin loading and release from PLL-grafted MSN samples.

3.3 PLL grafting of MSN-NH_2 and MSN-TETA

Often DDS show low biocompatibility and high cytotoxicity.[58–60] MSNs grafting with biopolymers, (i.e. PLL), could solve these issues and enhance DDS features.[24] PLL was grafted to MSN-NH_2 and MSN-TETA by mean of glutaraldehyde. To confirm PLL grafting TG analysis of MSN-PLL in comparison with MSN, MSN-NH_2 and MSN-TETA samples was performed. (see Fig. 2 and Table 2). In the temperature range 250°C - 700 °C, MSN-NH_2-PLL and MSN-TETA-PLL samples have mass losses of 20% and 27.4%, respectively, attributed to the combustion of PLL polymer. These values correspond to an amount of grafted PLL of 140.7 mg/g for MSN-TETA-PLL and of 100.3 mg/g for MSN-NH_2-PLL.

To further confirm PLL functionalization, zeta potentials (ζ) of bare, functionalized and PLL-grafted MSNs were measured as a function of pH (Fig. 4 and Supporting Information). MSN showed an isoelectric point pI = 4.1 while for MSN-NH_2 and for MSN-TETA it increased to pI = 8.0 and 9.2, respectively. The pI of amino functionalized MSNs occurs at a higher pH value because of the presence of positively charged (-NH_3^+) groups. MSN-NH_2-PLL and MSN-TETA-PLL show a further shift of the isoelectric point (pI = 8.3 and 9.8, respectively) due to the long cationic polymer chain of PLL (Table 2). This value of isoelectric point is slightly lower to those reported in literature (pI = 10-11)[61] confirming PLL functionalization.

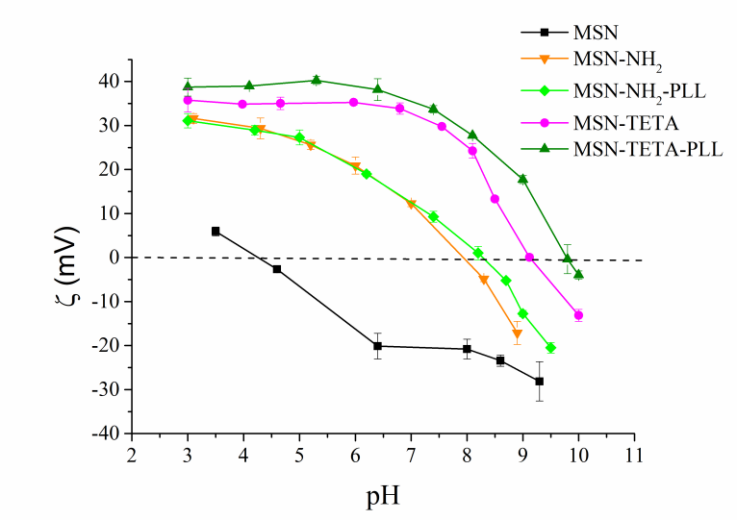

Figure 4. Zeta potential (ζ) as a function of pH in water for MSN, MSN-TETA, MSN-TETA- PLL, MSN-NH_2, and MSN-NH_2-PLL samples.

3.4 Quercetin loading and release from MSN-NH_2-PLL, MSN-TETA-PLL as function of pH

The obtained PLL-grafted MSN samples were then loaded with quercetin from a EtOH:H_2O 50:50 mixture. Quercetin loadings were 113.8 and 109.2 mg/g for MSN-NH_2-PLL and MSN-TETA-PLL, respectively. These values were slightly higher than those obtained for MSN-NH_2 (92.6 mg/g) and MSN-TETA (92.8 mg/g), likely due to the establishment of favorable interactions between quercetin and PLL chains. PLL is a pH responsive polymer that should change conformation going from neutral to acidic pH.[25,54] To evaluate the pH response of the DDS, the release of quercetin from MSN-NH_2-PLL and MSN-TETA-PLL was carried out at two different pH values, namely, pH = 7.4 and 3 in PBS buffer.

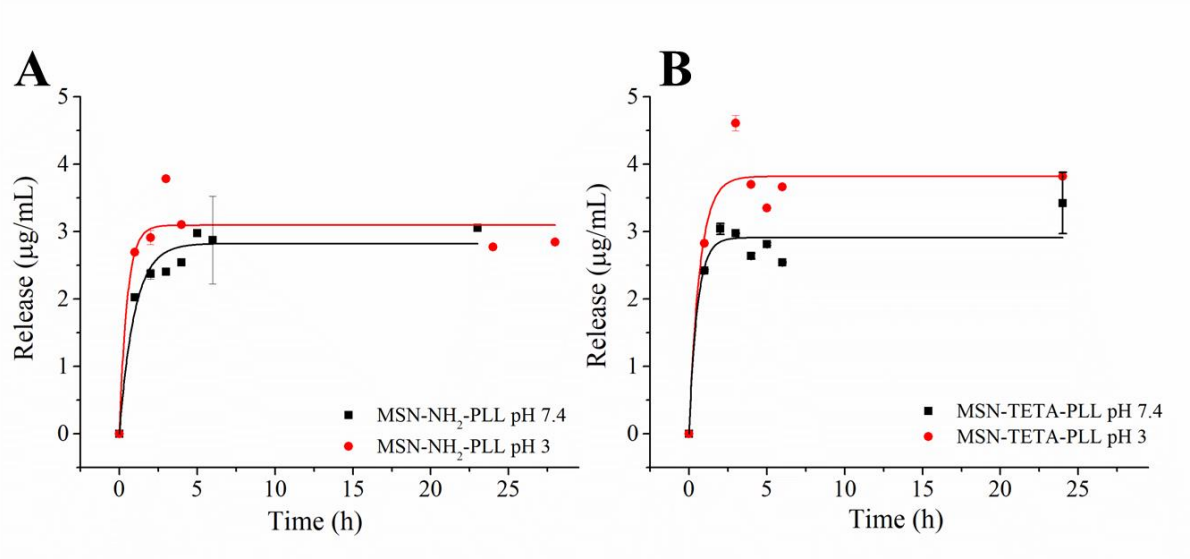

Figure 5. Quercetin release of A) MSN-NH_2-PLL and B) MSN-TETA-PLL at pH 3 and 7.4.

A change of pH should affect the maximal amount of released quercetin (A_{max}) because, in response to acidic pH, a conformation change of PLL should favor drug release.[62] However, in agreement with the slight change of zeta potential observed at pH 7.4 and 3, MSN-NH_2-PLL did not show a significant difference in pH response. Indeed, at pH 3 A_{max} = 2.6 µg/mL and 2.9 µg/mL at pH 7.4. Consistently with the change of zeta potential with pH, MSN-TETA-PLL was more sensitive to pH changes, resulting in A_{max} = 3.6 µg/mL and 2.8 µg/mL at pH = 3 and 7.4, respectively.[54]

Besides A_{max}, pH affects also k_1. Kinetic constants of quercetin release from MSN-NH_2-PLL decreases with decreasing pH from 2.6 h^{-1} at pH 7.4 to 1.3 h^{-1} at pH 3. Similarly, for MSN-TETA-PLL the kinetic constant decreases from pH 7.4 (1.7 h^{-1}) to pH 3 (1.5 h^{-1}). The decrease of k_1 suggests that quercetin interacts more strongly with PLL groups at acidic pH with a resulting slowdown of the release process. Quercetin molecule has 5 phenolic groups each having a different pK_a value (Table S1).[63,64] The first pK_a of quercetin measured by spectrophotometry is 6.74.[65] According to Diduk et al.[66] quercetin is only partially deprotonated at physiological pH 7.4.

At pH 7.4, the kinetic constants of both MSN-NH_2-PLL and MSN-TETA-PLL (2.9 and 2.8 h^{-1} respectively) are 15 times higher than the values found for MSN-NH_2 and MSN-TETA loaded at EtOH:H_2O 50:50 ratio (0.2 and 0.1 h^{-1} respectively) (Table 4). The higher k_1 values obtained for PLL-

grafted samples might be due to quercetin adsorption mainly on the external surface rather than within mesopores.

Table 4. Kinetic parameters release for MSN-NH_2-PLL and MSN-TETA-PLL at pH 3 and 7.4.

	MSN-NH_2-PLL				**MSN-TETA-PLL**			
	Loading (mg/g)	**A_{max} (µg/mL)**	**k_1 (h^{-1})**	**R^2**	**Loading (mg/g)**	**A_{max} (µg/mL)**	**k_1 (h^{-1})**	**R^2**
pH 7.4	113.8	2.9	2.6	0.99	109.2	2.8	1.8	0.99
pH 3	113.8	2.6	1.3	0.98	109.2	3.6	1.5	0.99

A successful DDS should release an amount of drug that matches drug concentration in plasma within a therapeutic window.[67,68] Kaushik et al. studied quercetin concentration in plasma after oral administration of quercetin aglycone using various food supplements such as quercetin fortified bars and chews.[69] Quercetin concentration in plasma ranged from 0.2 to 3 µg/mL.[69] It is noteworthy that for PLL grafted MSN samples in the present work, the maximal concentration of released quercetin matches the concentration of quercetin in plasma after oral administration.

3.5 Quercetin stability

Quercetin shows low chemical stability depending on pH.[70–73] For example Lei. et al.[72] studied quercetin degradation at basic pH with electrogenerated chemiluminescence. Zenchevich et al.[73] studied quercetin at basic and acidic pH through UV-Vis spectroscopy and HPLC to analyze quercetin oxidation products. In our work the stability of free quercetin (at a concentration of 2 µg/mL) in PBS was studied by means of UV-Vis spectroscopy. The UV-Vis spectrum of quercetin at pH 3 displays two main peaks at 255 and 370 nm with no substantial change as a function of time (Fig. 6A). The spectrum of a freshly prepared sample of quercetin at pH 7.4 is slightly different from that at pH 3, showing two main peaks at 255 nm and 375 nm and one small peak at 316 nm, consistently with what reported in literature.[74] However, after 6 h of incubation under physiological conditions (T = 37°C

and pH 7.4), quercetin solution showed a hypochromic shift. This band shift suggests a chemical change likely due to a loss of conjugation in slightly basic pH, as reported in literature.[75–79] More specifically at neutral and slightly basic pH values quercetin is rapidly oxidized.[80] It has been found that at alkaline conditions, the γ-pyrone fragment of quercetin decomposes with the formation of one isomer of a benzenetriol together with 2,4,6 trihydrobenzoic and 3,4 dihydroxybenzoic acid.[64,73] Fig.6 shows the UV-Vis of quercetin after release from PLL-grafted MSNs at different release times. At t = 6 h the UV-Vis spectrum of quercetin is exactly the same of that of the original molecule. According with UV-Vis spectra in Fig. 6D, quercetin is oxidized only after 24 h from the release by MSN-TETA-PLL at pH 7.4 and 37°C, thus indicating an improved storage stability of the drug immobilized on functionalized MSNs.

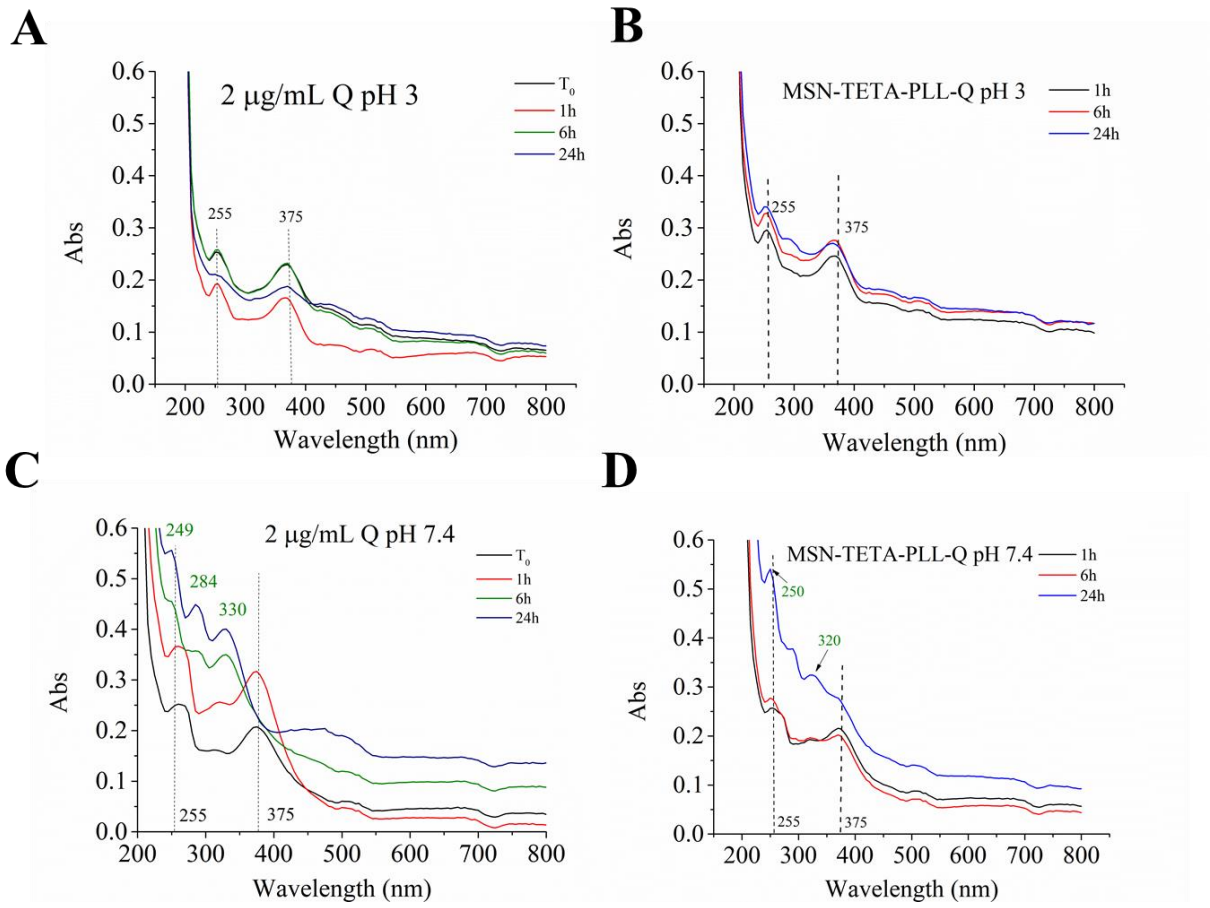

Figure 6. UV-Vis spectra of free quercetin at pH 3 A) and pH 7.4 spectra are reported as stack peaks to evaluate before (black values) and after degradation (green values) C) UV-Vis spectra of release quercetin solution from MSN-TETA-PLL pH 3 B) and pH 7.4 D) measured after different incubation times in PBS at 37 °C.

All functionalized samples, MSN-NH_2, MSN-TETA, MSN-NH_2-PLL (Fig. S2-S3) and MSN-TETA-PLL, have the same protective action toward quercetin molecule, thus they could guarantee the transport and release of unaltered quercetin at appropriate concentration.

4.Conclusions

In this work different functionalized mesoporous silica nanoparticles, MSN, MSN-NH_2 MSN-TETA, MSN-NH_2-PLL and MSN-TETA-PLL samples were synthesized as demonstrated by several characterization techniques. Quercetin, a natural antioxidant drug with anticancer and antimicrobial activity, was loaded on MSN, MSN-NH_2 and MSN-TETA at two different EtOH:H_2O ratios (80:20 and 50:50). Mixtures used in the loading step strongly influence A_{max} and k_1 with the best performance reported for EtOH:H_2O 50:50. Our findings suggest that adsorption promotes attractive interactions between quercetin and functionalized-MSN surface. Contrarily, impregnation does not produce any effective drug-carrier interactions thus resulting in a burst release once dispersed in aqueous solution. With the last solvent mixture, release kinetic constants followed the order of MSN > MSN-NH_2 > MSN-TETA (up to 0.1 h^{-1} for the lowest value with the most sustained release). This result suggests an additional influence of functionalization moiety on quercetin release. MSN-NH_2 and MSN-TETA samples were further functionalized with a cationic polymer, poly-L-lysine. PLL grafted MSN where then loaded with quercetin using 50:50 EtOH:H_2O mixture. With MSN-TETA PLL and MSN-NH_2-PLL, A_{max} laid in the range of 0.2 to 3 µg/mL, being in the same concentration range found in plasma after quercetin supplements assumption. Moreover, immobilization in functionalized MSN preserved quercetin stability avoiding its oxidation up to 6 h. The obtained DDS could guarantee the transport, the protection, and the release of native quercetin at the optimal concentration. Further work is in progress to evaluate the efficacy of these new promising DDS through different biological assays.

Acknowledgements

A.S. thanks L.R. 7 (CUP: J81G17000150002), FIR 2020 and Fondazione di Sardegna (FdS, F72F20000230007), M.M. thanks Regione Autonoma della Sardegna (RASSR79857) and C.C. thanks MIUR (PON-AIM Azione I.2–DD n. 407-27.02.2018, AIM1890410-2) for financial support.

References

(1) Nordström, R.; Malmsten, M. Delivery Systems for Antimicrobial Peptides. *Adv. Colloid Interface Sci.* **2017**, *242*, 17–34. https://doi.org/10.1016/j.cis.2017.01.005.

(2) Malekkhaiat Häffner, S.; Malmsten, M. Interplay between Amphiphilic Peptides and Nanoparticles for Selective Membrane Destabilization and Antimicrobial Effects. *Curr. Opin. Colloid Interface Sci.* **2019**, *44*, 59–71. https://doi.org/10.1016/j.cocis.2019.09.004.

(3) Nalwa, H. S. A Special Issue on Reviews in Nanomedicine, Drug Delivery and Vaccine Development. *J. Biomed. Nanotechnol.* **2014**, *10* (9), 1635–1640. https://doi.org/10.1166/jbn.2014.2033.

(4) Aslan, S.; Deneufchatel, M.; Hashmi, S.; Li, N.; Pfefferle, L. D.; Elimelech, M.; Pauthe, E.; Van Tassel, P. R. Carbon Nanotube-Based Antimicrobial Biomaterials Formed via Layer-by-Layer Assembly with Polypeptides. *J. Colloid Interface Sci.* **2012**, *388* (1), 268–273. https://doi.org/10.1016/j.jcis.2012.08.025.

(5) Abeer, M. M.; Rewatkar, P.; Qu, Z.; Talekar, M.; Kleitz, F.; Schmid, R.; Lindén, M.; Kumeria, T.; Popat, A. Silica Nanoparticles: A Promising Platform for Enhanced Oral Delivery of Macromolecules. *J. Control. Release* **2020**, *326* (July), 544–555. https://doi.org/10.1016/j.jconrel.2020.07.021.

(6) Cho, H.; Lai, T. C.; Tomoda, K.; Kwon, G. S. Polymeric Micelles for Multi-Drug Delivery in Cancer. *AAPS PharmSciTech* **2014**, *16* (1), 10–20. https://doi.org/10.1208/s12249-014-0251-

3.

(7) Hallaj-Nezhadi, S.; Hassan, M. Nanoliposome-Based Antibacterial Drug Delivery. *Drug Deliv.* **2015**, *22* (5), 581–589. https://doi.org/10.3109/10717544.2013.863409.

(8) Nizamov, T. R.; Garanina, A. S.; Grebennikov, I. S.; Zhironkina, O. A.; Strelkova, O. S.; Alieva, I. B.; Kireev, I. I.; Abakumov, M. A.; Savchenko, A. G.; Majouga, A. G. Effect of Iron Oxide Nanoparticle Shape on Doxorubicin Drug Delivery Toward LNCaP and PC-3 Cell Lines. *Bionanoscience* **2018**, *8* (1), 394–406. https://doi.org/10.1007/s12668-018-0502-y.

(9) Mas, N.; Galiana, I.; Mondragõn, L.; Aznar, E.; Climent, E.; Cabedo, N.; Sancenõn, F.; Murguía, J. R.; Martínez-Máñez, R.; Marcos, M. D.; Amorõs, P. Enhanced Efficacy and Broadening of Antibacterial Action of Drugs via the Use of Capped Mesoporous Nanoparticles. *Chem. - A Eur. J.* **2013**, *19* (34), 11167–11171. https://doi.org/10.1002/chem.201302170.

(10) Braun, K.; Pochert, A.; Lindén, M.; Davoudi, M.; Schmidtchen, A.; Nordström, R.; Malmsten, M. Membrane Interactions of Mesoporous Silica Nanoparticles as Carriers of Antimicrobial Peptides. *J. Colloid Interface Sci.* **2016**, *475*, 161–170. https://doi.org/10.1016/j.jcis.2016.05.002.

(11) Vallet-Regí, M.; Colilla, M.; Izquierdo-Barba, I.; Manzano, M. Mesoporous Silica Nanoparticles for Drug Delivery: Current Insights. *Molecules* **2018**, *23* (1), 1–19. https://doi.org/10.3390/molecules23010047.

(12) Salis, A.; Fanti, M.; Medda, L.; Nairi, V.; Cugia, F.; Piludu, M.; Sogos, V.; Monduzzi, M. Mesoporous Silica Nanoparticles Functionalized with Hyaluronic Acid and Chitosan Biopolymers. Effect of Functionalization on Cell Internalization. *ACS Biomater. Sci. Eng.* **2016**, *2* (5), 741–751. https://doi.org/10.1021/acsbiomaterials.5b00502.

(13) Nairi, V.; Magnolia, S.; Piludu, M.; Nieddu, M.; Caria, C. A.; Sogos, V.; Vallet-Regì, M.; Monduzzi, M.; Salis, A. Mesoporous Silica Nanoparticles Functionalized with Hyaluronic Acid. Effect of the Biopolymer Chain Length on Cell Internalization. *Colloids Surfaces B Biointerfaces* **2018**, *168*, 50–59. https://doi.org/10.1016/j.colsurfb.2018.02.019.

(14) Nairi, V.; Medda, L.; Monduzzi, M.; Salis, A. Adsorption and Release of Ampicillin Antibiotic from Ordered Mesoporous Silica. *J. Colloid Interface Sci.* **2017**, *497*, 217–225. https://doi.org/10.1016/j.jcis.2017.03.021.

(15) Magner, E. Immobilisation of Enzymes on Mesoporous Silicate Materials. *Chem. Soc. Rev.* **2013**, *42* (15), 6213–6222. https://doi.org/10.1039/c2cs35450k.

(16) Hsiao, I. L.; Fritsch-Decker, S.; Leidner, A.; Al-Rawi, M.; Hug, V.; Diabaté, S.; Grage, S. L.; Meffert, M.; Stoeger, T.; Gerthsen, D.; Ulrich, A. S.; Niemeyer, C. M.; Weiss, C. Biocompatibility of Amine-Functionalized Silica Nanoparticles: The Role of Surface Coverage. *Small* **2019**, *15* (10), 1–11. https://doi.org/10.1002/smll.201805400.

(17) Chaudhary, Z.; Subramaniam, S.; Khan, G. M.; Abeer, M. M.; Qu, Z.; Janjua, T.; Kumeria, T.; Batra, J.; Popat, A. Encapsulation and Controlled Release of Resveratrol Within Functionalized Mesoporous Silica Nanoparticles for Prostate Cancer Therapy. *Front. Bioeng. Biotechnol.* **2019**, *7* (September), 1–9. https://doi.org/10.3389/fbioe.2019.00225.

(18) Kierys, A.; Zaleski, R.; Grochowicz, M.; Gorgol, M.; Sienkiewicz, A. Polymer–Mesoporous Silica Composites for Drug Release Systems. *Microporous Mesoporous Mater.* **2020**, *294* (October 2019). https://doi.org/10.1016/j.micromeso.2019.109881.

(19) Kwon, S.; Singh, R. K.; Perez, R. A.; Neel, E. A. A.; Kim, H. W.; Chrzanowski, W. Silica-Based Mesoporous Nanoparticles for Controlled Drug Delivery. *J. Tissue Eng.* **2013**, *4* (1), 1–18. https://doi.org/10.1177/2041731413503357.

(20) Zaharudin, N. S.; Mohamed Isa, E. D.; Ahmad, H.; Abdul Rahman, M. B.; Jumbri, K.

Functionalized Mesoporous Silica Nanoparticles Templated by Pyridinium Ionic Liquid for Hydrophilic and Hydrophobic Drug Release Application. *J. Saudi Chem. Soc.* **2020**, *24* (3), 289–302. https://doi.org/10.1016/j.jscs.2020.01.003.

(21) Day, C. M.; Sweetman, M. J.; Song, Y.; Plush, S. E.; Garg, S. Applied Sciences Functionalized Mesoporous Silica Nanoparticles as Delivery Systems for Doxorubicin : Drug Loading and Release. **2021**, 14–16.

(22) Nairi, V.; Medda, S.; Piludu, M.; Casula, M. F.; Vallet-Regì, M.; Monduzzi, M.; Salis, A. Interactions between Bovine Serum Albumin and Mesoporous Silica Nanoparticles Functionalized with Biopolymers. *Chem. Eng. J.* **2018**, *340* (January), 42–50. https://doi.org/10.1016/j.cej.2018.01.011.

(23) Lin, C. Y.; Yang, C. M.; Lindén, M. Influence of Serum Concentration and Surface Functionalization on the Protein Adsorption to Mesoporous Silica Nanoparticles. *RSC Adv.* **2019**, *9* (58), 33912–33921. https://doi.org/10.1039/c9ra05585a.

(24) Patil, N. A.; Kandasubramanian, B. Functionalized Polylysine Biomaterials for Advanced Medical Applications: A Review. *Eur. Polym. J.* **2021**, *146* (November 2020), 110248. https://doi.org/10.1016/j.eurpolymj.2020.110248.

(25) Zheng, M.; Pan, M.; Zhang, W.; Lin, H.; Wu, S.; Lu, C.; Tang, S.; Liu, D.; Cai, J. Poly(α-L-Lysine)-Based Nanomaterials for Versatile Biomedical Applications: Current Advances and Perspectives. *Bioact. Mater.* **2021**, *6* (7), 1878–1909. https://doi.org/10.1016/j.bioactmat.2020.12.001.

(26) Shih, I.-; Van, Y.-; Shen, M.-. Biomedical Applications of Chemically and Microbiologically Synthesized Poly(Glutamic Acid) and Poly(Lysine). *Mini-Reviews Med. Chem.* **2005**, *4* (2), 179–188. https://doi.org/10.2174/1389557043487420.

(27) Manouchehri, S.; Zarrintaj, P.; Saeb, M. R.; Ramsey, J. D. Advanced Delivery Systems

Based on Lysine or Lysine Polymers. *Mol. Pharm.* **2021**, *18* (10), 3652–3670. https://doi.org/10.1021/acs.molpharmaceut.1c00474.

(28) Lio, D. C. S.; Liu, C.; Oo, M. M. S.; Wiraja, C.; Teo, M. H. Y.; Zheng, M.; Chew, S. W. T.; Wang, X.; Xu, C. Transdermal Delivery of Small Interfering RNAs with Topically Applied Mesoporous Silica Nanoparticles for Facile Skin Cancer Treatment. *Nanoscale* **2019**, *11* (36), 17041–17051. https://doi.org/10.1039/c9nr06303j.

(29) Hartono, S. B.; Gu, W.; Kleitz, F.; Liu, J.; He, L.; Middelberg, A. P. J.; Yu, C.; Lu, G. Q.; Qiao, S. Z. Poly-L-Lysine Functionalized Large Pore Cubic Mesostructured Silica Nanoparticles as Biocompatible Carriers for Gene Delivery. *ACS Nano* **2012**, *6* (3), 2104–2117. https://doi.org/10.1021/nn2039643.

(30) Dai, X.; Ma, J.; Chen, N.; Cai, Y.; He, Y.; Li, X.; Gao, F. MSNs-Based Nanocomposite for Biofilm Imaging and NIR-Activated Chem/Photothermal/Photodynamic Combination Therapy. *ACS Appl. Bio Mater.* **2021**, *4* (3), 2810–2820. https://doi.org/10.1021/acsabm.1c00034.

(31) Mohammed, S. A. A.; Khan, R. A.; El-readi, M. Z.; Emwas, A. H.; Sioud, S.; Poulson, B. G.; Jaremko, M.; Eldeeb, H. M.; Al-omar, M. S.; Mohammed, H. A. Suaeda Vermiculata Aqueous-ethanolic Extract-based Mitigation of Ccl4-induced Hepatotoxicity in Rats, and Hepg-2 and Hepg-2/Adr Cell-lines-based Cytotoxicity Evaluations. *Plants* **2020**, *9* (10), 1–26. https://doi.org/10.3390/plants9101291.

(32) El-Saber Batiha, G.; Beshbishy, A. M.; Ikram, M.; Mulla, Z. S.; Abd El-Hack, M. E.; Taha, A. E.; Algammal, A. M.; Ali Elewa, Y. H. The Pharmacological Activity, Biochemical Properties, and Pharmacokinetics of the Major Natural Polyphenolic Flavonoid: Quercetin. *Foods* **2020**, *9* (3). https://doi.org/10.3390/foods9030374.

(33) Sato, S.; Mukai, Y. Modulation of Chronic Inflammation by Quercetin: The Beneficial

Effects on Obesity. *J. Inflamm. Res.* **2020**, *13*, 421–431. https://doi.org/10.2147/JIR.S228361.

(34) Vafadar, A.; Shabaninejad, Z.; Movahedpour, A.; Fallahi, F.; Taghavipour, M.; Ghasemi, Y.; Akbari, M.; Shafiee, A.; Hajighadimi, S.; Moradizarmehri, S.; Razi, E.; Savardashtaki, A.; Mirzaei, H. Quercetin and Cancer: New Insights into Its Therapeutic Effects on Ovarian Cancer Cells. *Cell Biosci.* **2020**, *10* (1), 1–17. https://doi.org/10.1186/s13578-020-00397-0.

(35) Xu, D.; Hu, M. J.; Wang, Y. Q.; Cui, Y. L. Antioxidant Activities of Quercetin and Its Complexes for Medicinal Application. *Molecules* **2019**, *24* (6). https://doi.org/10.3390/molecules24061123.

(36) Jaisinghani, R. N. Antibacterial Properties of Quercetin. *Microbiol. Res. (Pavia).* **2017**, *8* (1). https://doi.org/10.4081/mr.2017.6877.

(37) Badshah, S. L.; Faisal, S.; Muhammad, A.; Poulson, B. G.; Emwas, A. H.; Jaremko, M. Antiviral Activities of Flavonoids. *Biomed. Pharmacother.* **2021**, *140* (March), 111596. https://doi.org/10.1016/j.biopha.2021.111596.

(38) Yang, D.; Wang, T.; Long, M.; Li, P. Quercetin: Its Main Pharmacological Activity and Potential Application in Clinical Medicine. *Oxid. Med. Cell. Longev.* **2020**, *2020*. https://doi.org/10.1155/2020/8825387.

(39) Wang, Y.; Tao, B.; Wan, Y.; Sun, Y.; Wang, L.; Sun, J.; Li, C. Drug Delivery Based Pharmacological Enhancement and Current Insights of Quercetin with Therapeutic Potential against Oral Diseases. *Biomed. Pharmacother.* **2020**, *128* (May), 110372. https://doi.org/10.1016/j.biopha.2020.110372.

(40) Wang, S.; Yao, J.; Zhou, B.; Yang, J.; Chaudry, M. T.; Wang, M.; Xiao, F.; Li, Y.; Yin, W. Bacteriostatic Effect of Quercetin as an Antibiotic Alternative in Vivo and Its Antibacterial Mechanism in Vitro. *J. Food Prot.* **2018**, *81* (1), 68–78. https://doi.org/10.4315/0362-

028X.JFP-17-214.

(41) Gao, L.; Liu, G.; Wang, X.; Liu, F.; Xu, Y.; Ma, J. Preparation of a Chemically Stable Quercetin Formulation Using Nanosuspension Technology. *Int. J. Pharm.* **2011**, *404* (1–2), 231–237. https://doi.org/10.1016/j.ijpharm.2010.11.009.

(42) E.A. AbouAitah, K.; A. Farghali, A. Mesoporous Silica Materials in Drug Delivery System: PH/Glutathione- Responsive Release of Poorly Water-Soluble Pro-Drug Quercetin from Two and Three-Dimensional Pore-Structure Nanoparticles. *J. Nanomed. Nanotechnol.* **2016**, *07* (02). https://doi.org/10.4172/2157-7439.1000360.

(43) Scalia, S.; Mezzena, M. Incorporation of Quercetin in Lipid Microparticles: Effect on Photo- and Chemical-Stability. *J. Pharm. Biomed. Anal.* **2009**, *49* (1), 90–94. https://doi.org/10.1016/j.jpba.2008.10.011.

(44) Ugazio, E.; Gastaldi, L.; Brunella, V.; Scalarone, D.; Jadhav, S. A.; Oliaro-Bosso, S.; Zonari, D.; Berlier, G.; Miletto, I.; Sapino, S. Thermoresponsive Mesoporous Silica Nanoparticles as a Carrier for Skin Delivery of Quercetin. *Int. J. Pharm.* **2016**, *511* (1), 446–454. https://doi.org/10.1016/j.ijpharm.2016.07.024.

(45) Berlier, G.; Gastaldi, L.; Ugazio, E.; Miletto, I.; Iliade, P.; Sapino, S. Stabilization of Quercetin Flavonoid in MCM-41 Mesoporous Silica: Positive Effect of Surface Functionalization. *J. Colloid Interface Sci.* **2013**, *393* (1), 109–118. https://doi.org/10.1016/j.jcis.2012.10.073.

(46) Sapino, S.; Ugazio, E.; Gastaldi, L.; Miletto, I.; Berlier, G.; Zonari, D.; Oliaro-Bosso, S. Mesoporous Silica as Topical Nanocarriers for Quercetin: Characterization and in Vitro Studies. *Eur. J. Pharm. Biopharm.* **2015**, *89*, 116–125. https://doi.org/10.1016/j.ejpb.2014.11.022.

(47) Sarkar, A.; Ghosh, S.; Chowdhury, S.; Pandey, B.; Sil, P. C. Targeted Delivery of Quercetin

Loaded Mesoporous Silica Nanoparticles to the Breast Cancer Cells. *Biochim. Biophys. Acta - Gen. Subj.* **2016**, *1860* (10), 2065–2075. https://doi.org/10.1016/j.bbagen.2016.07.001.

(48) Ghanimati, M.; Jabbari, M.; Farajtabar, A.; Nabavi-Amri, S. A. Adsorption Kinetics and Isotherms of Bioactive Antioxidant Quercetin onto Amino-Functionalized Silica Nanoparticles in Aqueous Ethanol Solutions. *New J. Chem.* **2017**, *41* (16), 8451–8458. https://doi.org/10.1039/c7nj01489a.

(49) Rubini, K.; Boanini, E.; Menichetti, A.; Bonvicini, F.; Gentilomi, G. A.; Montalti, M.; Bigi, A. Quercetin Loaded Gelatin Films with Modulated Release and Tailored Anti-Oxidant, Mechanical and Swelling Properties. *Food Hydrocoll.* **2020**, *109* (March), 106089. https://doi.org/10.1016/j.foodhyd.2020.106089.

(50) Kazakova, O. A.; Gun'ko, V. M.; Lipkovskaya, N. A.; Voronin, E. F.; Pogorelyi, V. K. Interaction of Quercetin with Highly Dispersed Silica in Aqueous Suspensions. *Colloid J.* **2002**, *64* (4), 412–418. https://doi.org/10.1023/A:1016807717891.

(51) Islami, M.; Zarrabi, A.; Tada, S.; Kawamoto, M.; Isoshima, T.; Ito, Y. Controlled Quercetin Release from High-Capacity-Loading Hyperbranched Polyglycerol-Functionalized Graphene Oxide. *Int. J. Nanomedicine* **2018**, *13*, 6059–6071. https://doi.org/10.2147/IJN.S178374.

(52) Lee, D.-H.; Sim, G.-S.; Kim, J.-H.; Lee, G.-S.; Pyo, H.-B.; Lee, B.-C. Preparation and Characterization of Quercetin-Loaded Polymethyl Methacrylate Microcapsules Using a Polyol-in-Oil-in-Polyol Emulsion Solvent Evaporation Method. *J. Pharm. Pharmacol.* **2010**, *59* (12), 1611–1620. https://doi.org/10.1211/jpp.59.12.0002.

(53) Steri, D.; Monduzzi, M.; Salis, A. Ionic Strength Affects Lysozyme Adsorption and Release from SBA-15 Mesoporous Silica. *Microporous Mesoporous Mater.* **2013**, *170*, 164–172. https://doi.org/10.1016/j.micromeso.2012.12.002.

(54) Lee, N.-K.; Park, S. S.; Ha, C.-S. PH-Sensitive Drug Delivery System Based on Mesoporous

Silica Modified with Poly-L-Lysine (PLL) as a Gatekeeper. *J. Nanosci. Nanotechnol.* **2020**, *20* (11), 6925–6934. https://doi.org/10.1166/jnn.2020.18821.

(55) Gonçalves, J. L. M.; Lopes, A. B. C.; Baleizão, C.; Farinha, J. P. S. Mesoporous Silica Nanoparticles Modified inside and out for on:Off Ph-Modulated Cargo Release. *Pharmaceutics* **2021**, *13* (5). https://doi.org/10.3390/pharmaceutics13050716.

(56) Beck, J. S.; Vartuli, J. C.; Roth, W. J.; Leonowicz, M. E.; Kresge, C. T.; Schmitt, K. D.; Chu, C. T. W.; Olson, D. H.; Sheppard, E. W.; McCullen, S. B.; Higgins, J. B.; Schlenker, J. L. A New Family of Mesoporous Molecular Sieves Prepared with Liquid Crystal Templates. *J. Am. Chem. Soc.* **1992**, *114* (27), 10834–10843. https://doi.org/10.1021/ja00053a020.

(57) Trendafilova, I.; Szegedi, A.; Mihály, J.; Momekov, G.; Lihareva, N.; Popova, M. Preparation of Efficient Quercetin Delivery System on Zn-Modified Mesoporous SBA-15 Silica Carrier. *Mater. Sci. Eng. C* **2017**, *73*, 285–292. https://doi.org/10.1016/j.msec.2016.12.063.

(58) Hudson, S. P.; Padera, R. F.; Langer, R.; Kohane, D. S. The Biocompatibility of Mesoporous Silicates. *Biomaterials* **2008**, *29* (30), 4045–4055. https://doi.org/10.1016/j.biomaterials.2008.07.007.

(59) Kohane, D. S.; Langer, R. Biocompatibility and Drug Delivery Systems. *Chem. Sci.* **2010**, *1* (4), 441–446. https://doi.org/10.1039/c0sc00203h.

(60) Naahidi, S.; Jafari, M.; Edalat, F.; Raymond, K.; Khademhosseini, A.; Chen, P. Biocompatibility of Engineered Nanoparticles for Drug Delivery. *J. Control. Release* **2013**, *166* (2), 182–194. https://doi.org/10.1016/j.jconrel.2012.12.013.

(61) Batys, P.; Morga, M.; Bonarek, P.; Sammalkorpi, M. PH-Induced Changes in Polypeptide Conformation: Force-Field Comparison with Experimental Validation. *J. Phys. Chem. B* **2020**, *124* (14), 2961–2972. https://doi.org/10.1021/acs.jpcb.0c01475.

(62) Yang, C.; Shi, Z.; Feng, C.; Li, R.; Luo, S.; Li, X.; Ruan, L. An Adjustable PH-Responsive Drug Delivery System Based on Self-Assembly Polypeptide-Modified Mesoporous Silica. *Macromol. Biosci.* **2020**, *20* (6), 1–10. https://doi.org/10.1002/mabi.202000034.

(63) Li, Z.; Moalin, M.; Zhang, M.; Vervoort, L.; Hursel, E.; Mommers, A.; Haenen, G. R. M. M. The Flow of the Redox Energy in Quercetin during Its Antioxidant Activity in Water. *Int. J. Mol. Sci.* **2020**, *21* (17), 1–16. https://doi.org/10.3390/ijms21176015.

(64) Chebotarev, A. N.; Snigur, D. V. Study of the Acid-Base Properties of Quercetin in Aqueous Solutions by Color Measurements. *J. Anal. Chem.* **2015**, *70* (1), 55–59. https://doi.org/10.1134/S1061934815010062.

(65) Jovanovic, S. V.; Steenken, S.; Tosic, M.; Marjanovic, B.; Simic, M. G. Flavonoids as Antioxidants. *J. Am. Chem. Soc.* **1994**, *116* (11), 4846–4851. https://doi.org/10.1021/ja00090a032.

(66) Álvarez-Diduk, R.; Ramírez-Silva, M. T.; Galano, A.; Merkoçi, A. Deprotonation Mechanism and Acidity Constants in Aqueous Solution of Flavonols: A Combined Experimental and Theoretical Study. *J. Phys. Chem. B* **2013**, *117* (41), 12347–12359. https://doi.org/10.1021/jp4049617.

(67) Vargason, A. M.; Anselmo, A. C.; Mitragotri, S. The Evolution of Commercial Drug Delivery Technologies. *Nat. Biomed. Eng.* **2021**, *5* (9), 951–967. https://doi.org/10.1038/s41551-021-00698-w.

(68) Adepu, S.; Ramakrishna, S. Controlled Drug Delivery Systems: Current Status and Future Directions. *Molecules* **2021**, *26* (19). https://doi.org/10.3390/molecules26195905.

(69) Kaushik, D.; O'Fallon, K.; Clarkson, P. M.; Patrick Dunne, C.; Conca, K. R.; Michniak-Kohn, B. Comparison of Quercetin Pharmacokinetics Following Oral Supplementation in Humans. *J. Food Sci.* **2012**, *77* (11). https://doi.org/10.1111/j.1750-3841.2012.02934.x.

(70) Wang, W.; Sun, C.; Mao, L.; Ma, P.; Liu, F.; Yang, J.; Gao, Y. The Biological Activities, Chemical Stability, Metabolism and Delivery Systems of Quercetin: A Review. *Trends Food Sci. Technol.* **2016**, *56*, 21–38. https://doi.org/10.1016/j.tifs.2016.07.004.

(71) Moon, Y.J., Wang, L., DiCenzo, R. and Morris, M. E. Quercetin Pharmacokinetics in Humans. *Biopharm. Drug Dispos.* **2008**, *29* (3), 205–217. https://doi.org/doi.org/10.1002/bdd.605.

(72) Lei, R.; Xu, X.; Yu, F.; Li, N.; Liu, H. W.; Li, K. A Method to Determine Quercetin by Enhanced Luminol Electrogenerated Chemiluminescence (ECL) and Quercetin Autoxidation. *Talanta* **2008**, *75* (4), 1068–1074. https://doi.org/10.1016/j.talanta.2008.01.010.

(73) Zenkevich, I. G.; Eshchenko, A. Y.; Makarova, S. V.; Vitenberg, A. G.; Dobryakov, Y. G.; Utsal, V. A. Identification of the Products of Oxidation of Quercetin by Air Oxygen at Ambient Temperature. *Molecules* **2007**, *12* (3), 654–672. https://doi.org/10.3390/12030654.

(74) Ravichandran, R.; Rajendran, M.; Devapiriam, D. Antioxidant Study of Quercetin and Their Metal Complex and Determination of Stability Constant by Spectrophotometry Method. *Food Chem.* **2014**, *146*, 472–478. https://doi.org/10.1016/j.foodchem.2013.09.080.

(75) Biler, M.; Biedermann, D.; Valentová, K.; Křen, V.; Kubala, M. Quercetin and Its Analogues: Optical and Acido-Basic Properties. *Phys. Chem. Chem. Phys.* **2017**, *19* (39), 26870–26879. https://doi.org/10.1039/c7cp03845c.

(76) Jurasekova, Z.; Domingo, C.; Garcia-Ramos, J. V.; Sanchez-Cortes, S. Effect of PH on the Chemical Modification of Quercetin and Structurally Related Flavonoids Characterized by Optical (UV-Visible and Raman) Spectroscopy. *Phys. Chem. Chem. Phys.* **2014**, *16* (25), 12802–12811. https://doi.org/10.1039/c4cp00864b.

(77) Jurasekova, Z.; Torreggiani, A.; Tamba, M.; Sanchez-Cortes, S.; Garcia-Ramos, J. V. Raman and Surface-Enhanced Raman Scattering (SERS) Investigation of the Quercetin Interaction

with Metals: Evidence of Structural Changing Processes in Aqueous Solution and on Metal Nanoparticles. *J. Mol. Struct.* **2009**, *918* (1–3), 129–137. https://doi.org/10.1016/j.molstruc.2008.07.025.

(78) Kellil, A.; Grigorakis, S.; Loupassaki, S.; Makris, D. P. Empirical Kinetic Modelling and Mechanisms of Quercetin Thermal Degradation in Aqueous Model Systems: Effect of PH and Addition of Antioxidants. *Appl. Sci.* **2021**, *11* (6). https://doi.org/10.3390/app11062579.

(79) Golonka, I.; Wilk, S.; Musiał, W. The Influence of UV Radiation on the Degradation of Pharmaceutical Formulations Containing Quercetin. *Molecules* **2020**, *25* (22). https://doi.org/10.3390/molecules25225454.

(80) Mocek, B. M.; Richardson, P. J.; Breweries, C.; West, L. A. Kinetics and Mechanism of Quercetin Oxidation. **1972**, *78*.